

# A Computationally Efficient Semi-Analytical Method for Circulating Current Loss of High Speed Permanent Magnet Machines

Lei Li, Xinggong Fan, *Member, IEEE*, Zirui Liu, Dawei Li, *Senior Member, IEEE*, Tianjie Zou, Xiaoxue Chen, and Ronghai Qu, *Fellow, IEEE*

**Abstract**—This paper proposes a computationally efficient (CE) semi-analytical method for winding power loss calculation of high speed permanent magnet machines induced by circulating current. It combines a CE magnetostatic finite element method (FEM) for rapid slot leakage field extraction and an analytical circuit model for circulating current calculation. Time-space transformation based CE FEM is applied for efficient slot leakage field extraction considering the polyphase windings. Besides, a conductor model with an automatic and practical turn splitting strategy is proposed to consider the effect of conductor positions and bundle shapes on the circulating current loss. The results on circulating current waveforms and corresponding losses show that the proposed method has high accuracy and can significantly reduce the simulation time, with an error less than 2% and the simulation time only 1/400 for the studied machine compared with the commercial FEM. Using the proposed method, the influence of some factors, including the turn number, the transposition effect and the bundle shape on the circulating current loss are investigated. Finally, the proposed method is further verified by experimental measurements implemented on two stator specimens.

**Index Terms**—Computationally efficient (CE) FEM, permanent magnet (PM) machines, slot leakage extraction, circulating current, AC copper loss.

## I. INTRODUCTION

Due to ambitious roadmaps set on boosting power density level of electrical power-trains, development of permanent magnet (PM) machines towards ever higher rotation speed is an inevitable trend in many industrial sectors such as automotive traction and aircraft propulsion [1] [2]. Meanwhile, the resultant high fundamental frequency of winding current may lead to significant AC copper loss due to the skin and proximity effect [3]. The generated AC copper loss can be very high and non-uniformly distributed within the slot, which poses a serious threat to the thermal and insulation reliability of winding system and should be carefully dealt with at machine design stage.

AC copper loss can be divided into the eddy current loss within the strands (strand-level loss) and circulating current loss among the parallel strands (bundle-level loss). For high-speed PM machines, the multistranded bundles with small copper wires are often used to effectively suppress the strand-level loss. On the other hand, circulating current based loss component can be significant and even dominant in the total winding loss [4-6]. Due to the large number of strands and the

complex slot leakage field in the slot, the calculation of the circulating current loss is a time-consuming process, which brings challenges to the machine design and optimization process. Hence, it is of significance to quickly and accurately evaluate the circulating current loss.

Based on existing research work in academia, circulating current issue can be investigated based on finite element method (FEM) [4] [7-11], analytical methods [12-16], and the semi-analytical methods [17-20].

Among the three methods, FEM is considered as the most accurate one due to its capability of modelling the complex slot leakage field with local magnetic saturation and the fringing effect taken into account. However, the FEM based method requires accurate modeling of individual conductors in the slot, which could result in large amount of meshes, especially when the conductors are small and their number is high. Moreover, in order to reflect the connection layout between conductors, the geometric modelling needs to be further combined with an external circuit with high number of elements. Hence, the FEM based method needs a cumbersome process at modelling stage, and is lack of universality along with. Moreover, the transient field-circuit coupling simulation, together with the large number of meshes, will significantly increase the computation cost, which makes this method not suitable for large-scale machine optimization.

To overcome the disadvantage of long calculation time of FEM, analytical methods [12-16] have been proposed to evaluate AC copper loss. The analytical method obtains the slot leakage field by directly solving the Maxwell's equations in the slot, and ultimately derives the circulating current in the strands through the analytical circuit model [12-14] or directly calculates the AC losses based on the Poynting's theorem [15] [16]. However, some assumptions and simplification, such as the neglect of magnetic saturation and simplification of the slot-winding geometry, usually have to be made before derivation the analytical equations. These assumptions and simplification will limit the calculation accuracy, especially when the machine is overloaded or the slot geometry is complex.

The semi-analytical method combines the advantages of the two methods above. It depends on the FEM to calculate the field information and the analytical circuit model to calculate the circulating current [17-20]. Therefore, the semi-analytical method decouples the calculations of the slot leakage field and the induced strand circulating currents. In

this case, the detailed FEM model is replaced by the simplified one without the need of modeling the numerous strands, which can significantly reduce the computation cost [3]. However, the existing semi-analytical methods are mostly based on 2-D or 3-D FEM over a full electrical period, which makes them less attractive in terms of computation speed compared to the analytical one. Besides, how the conductors are appropriately arranged in the slot, split into the turns and connected in the circuit model still bothers the researchers. A fully automatic and practical conductor model and connection process is worth being developed in order to effectively include parametric slot geometry and different winding patterns at machine design stage. Only in this way could the circulating current issue be reasonably considered in large-scale machine optimization.

In this paper, a CE semi-analytical method is proposed to calculate the circulating current loss based on the 2D magnetostatic CE FEM and an equivalent circuit model. Time-space transformation based CE FEM is first applied to calculate the slot leakage field considering the polyphase winding. Besides, a conductor model with an automatic and practical turn splitting strategy is proposed to establish a more actual circuit model. These improvements will significantly reduce the simulation time while achieving accurate results.

The structure of rest content is organized as follows. In Section II, the studied machine and the conventional FEA model for circulating loss calculation will be introduced. Then, the proposed CE semi-analytical method will be presented in Section III, with particular emphasis on the CE FEM and turn splitting strategy. Also, the results will be discussed and compared with the commercial FEM. In Section IV, some influence factors of circulating current loss including the different bundle/turn combinations, the transposition technique and the bundle shape will be studied using the proposed method. Finally, two stator specimens will be built to further verify the proposed method.

## II. STUDIED MACHINE AND FEA MODEL

In this paper, a 48-slot 4-pole, 200kW and 54000rpm high-speed permanent magnet machine with distributed winding has been selected as case study for the illustration of the proposed method. Two sets of windings A-B-C and U-V-W with corresponding phase axis shifted by  $\pi/6$  are configured in this machine.

TABLE I  
MAIN PARAMETERS OF THE PMSM

Parameters	Values
Rated power (kW)	200
DC bus voltage(V)	350
Number of slots	48
Number of poles	4
Rated speed (rpm)	54000
Stator outer diameter (mm)	222
Stator inner diameter (mm)	104
Core length (mm)	130
Number of phases	6
Number of parallel branches	4
Strand diameter (mm)	0.8
Slot filling factor	0.35

Table I shows the main parameters of the machine, and the vector diagram of the slot's electrical potential is shown in Fig. 1. Parallel-strand is used to reduce the eddy current loss in the winding at high speed operations. However, as a result of the uneven of the slot leakage magnetic field, circulating currents are induced between the parallel strands, leading to circulating current loss.

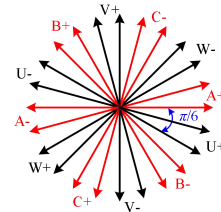


Fig. 1. Vector diagram of the slot's electrical potential.

Commercial FEM is usually used to calculate the circulating current loss. The conductors in slots need to be modeled based on practical consideration, with respect to their locations and sizes. Considering the symmetry of the machine, only the conductors of a parallel branch in one-phase are modeled to reduce the calculation time. For the studied machine, two series coils should be modeled and the indexes of the conductors are shown in Fig. 2(a). There are 4 turns (marked with 4 different colors) in each coil and 23 parallel strands in each parallel branch. To reflect the connection relationship between parallel strands, an external circuit is further built, including power source and windings. Considering the influence of the end-winding on the circulating current, the end-winding is equivalent to a DC resistance and connected in series the circuit, which is shown in Fig. 2(b). Although the pure FEM-based analysis method for circulating current might be accurate, it is very time-consuming, and may even become impossible when the number of mesh nodes exceeds a certain limit due to a large number of conductors.

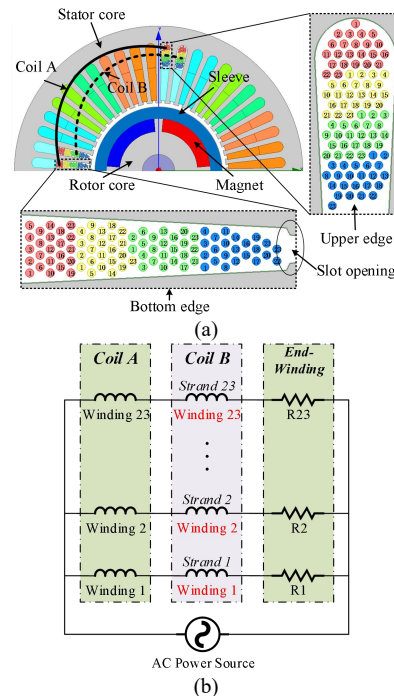


Fig. 2. (a) 2-D FEA model of the studied machine and (b) the external circuit.

### III. COMPUTATIONALLY EFFICIENT SEMI-ANALYTICAL METHOD FOR CIRCULATING CURRENT LOSS EVALUATION

In this section, a computationally efficient semi-analytical method is proposed for circulating current loss evaluation. It is based on the open source finite element software FEMM [21] and MATLAB [22] platform to realize the rapid calculation of the circulating currents among the parallel strands [3]. FEMM is a toolbox in MATLAB that solves the electromagnetic field using magnetostatic finite element method. MATLAB can be used to invoke the FEMM code package to solve the electromagnetic field and extract the magnetic information for post-processing of electromagnetic performance.

The proposed CE semi-analytical method adopts the FEMM to solve the electromagnetic field, and the analytical method to calculate the current of each parallel strand. When solving electromagnetic field, the simple model and the CE FEM are used to improve the computing efficiency. On the one hand, the simple model avoids the need for detailed modeling of a large number of conductors, **resulting in fewer divided meshes**. On the other hand, the CE FEM can reduce the number of simulation steps based on the time-space transformation. Their combination will greatly improve the computing efficiency.

To implement the proposed CE semi-analytical method, some assumptions are made as follows:

- Since the conductor diameter is much smaller than the axial size of the machine, the conductor in the slot is assumed infinitely long, such that the end effect can be ignored.
- The influence of non-uniform current distribution in conductor on the distribution of slot leakage magnetic field is negligible.
- Due to the small diameter of the conductor, the vector potential is linearly distributed on the conductor section, such that the flux leakage of the conductor can be approximated to the product of the vector potential at the conductor center and the length of active part of conductor.

Based on these assumptions, the circulating current loss can be calculated using the proposed method and the flowchart is depicted in Fig. 3:

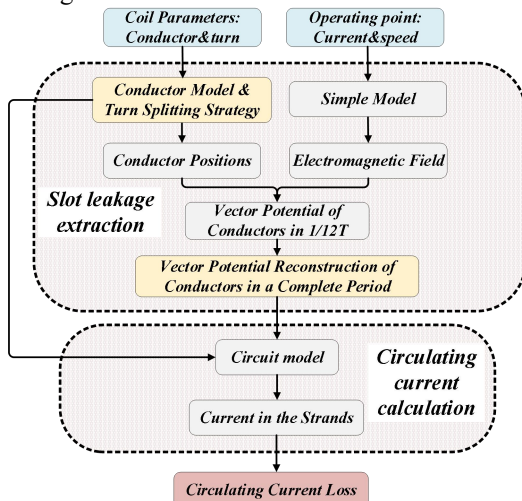


Fig. 3. The flowchart of the proposed method.

1) Firstly, the simple model and the conductor model considering the practical situation are established according to the

coil parameters (conductor and turn number) and the operating point (current and speed).

2) Secondly, using the CE FEM, the slot leakage of the full period is reconstructed based on the calculation field results of a short period of time and the conductor positions.

3) Finally, the slot leakage field will be substituted into an equivalent analytical circuit model to solve the current of each parallel strand, thus the circulating current loss can be obtained.

**In the following pages**, the conductor model with a practical turn splitting strategy, the CE FEM for polyphase winding and the newly derived analytical circuit model of the circulating current loss will be introduced in detail.

#### A. Conductor Model and Turn Splitting Strategy

In order to calculate the circulating current loss, a conductor model should be established. For the studied machine, an algorithm is used to lay out the conductor. First, a **base** conductor is placed at the bottom of the slot, then the others are laid out row by row from the slot bottom to the slot opening. Any three conductor centers are connected into an equilateral triangle, **allowing for the placement of more conductors**, as shown in Fig. 4. The wire insulation, conductor separation, liner and the coil divider are also taken into account in the conductor model, which makes it closer to the actual situation. The conductor model provides a convenient and efficient to obtain the position information of each conductor and can be used to calculate the circulating current loss combining the proposed method subsequently.

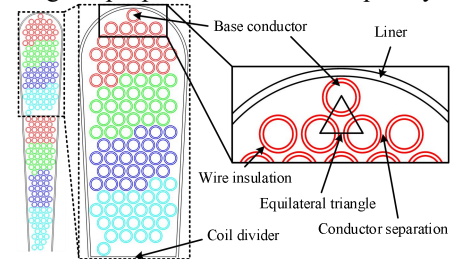


Fig. 4. Illustration of the conductor model.

For the studied machine, the parallel strands in the same turn and the distribution of the turns in one coil are shown in Fig. 2(a). The parallel strands numbered 1-23 in each turn are circumferentially arranged from the top to the bottom, and from the left to the right in the slot, which is one of the simplest turn splitting strategy. However, for the machine with wider slots or concentrated windings, the turn distribution is not appropriate on account that conductors in the same turn usually tend to be more concentrated. Previous studies have demonstrated the significant influence of bundle shape on circulating current loss. Three different arrangements are typically studied: **tangential arrangement (best)**, **the bundle arrangement (medium)** and **the radial arrangement (worst)**, in which the bundle one is regarded as the most practical arrangement [20]. Based on the conductor model, a new turn splitting strategy is proposed to be as similar as possible to the actual situation of the conductors in the slot as shown in Fig. 5. The strategy is implemented as follows, and the flowchart is shown in Fig. 6: (Assume that there are  $n$  conductors in one slot, which need to be divided into  $k$  turns)

- 1) Randomly select turn centers for turn center initialization.
  - 2) Calculate the distance between each conductor and each turn center.
  - 3) Assign each conductor to the nearest turn, and as long as the sum of squares of the distance between the conductor in the turn and the center can be reduced by reallocating the conductor to another center, this distribution is performed on the conductor.
  - 4) Calculate the average value of the conductor coordinates for each turn to obtain  $k$  new centroid locations.
  - 5) Repeat steps 2 to 4 until turn assignments do not change, or the maximum number of iterations is reached.
- Although the above process has completed the turn division of the conductor in the slot, the number of conductors in each turn is usually not equal. To make the number of conductors in each turn the same, carry out the following process:
- 6) Expand the matrix containing  $k$  center point coordinates to  $n$  center points, which means that  $n/k$  coordinates are copied for each coordinate and obtain a new center matrix.
  - 7) Calculate the distance between each conductor and the new center matrix, and obtain a  $n \times n$  matrix.
  - 8) The bipartite matching algorithm [23] is used to assign conductors so that the number of conductors in each turn is the same.
  - 9) Calculate the average value of the conductor coordinates for each turn to obtain new centroid locations.
  - 10) Repeat steps 6 to 9 until turn assignments do not change, or the maximum number of iterations is reached.

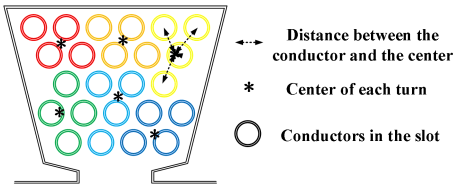


Fig. 5. The turn distribution of the proposed turn splitting strategy.

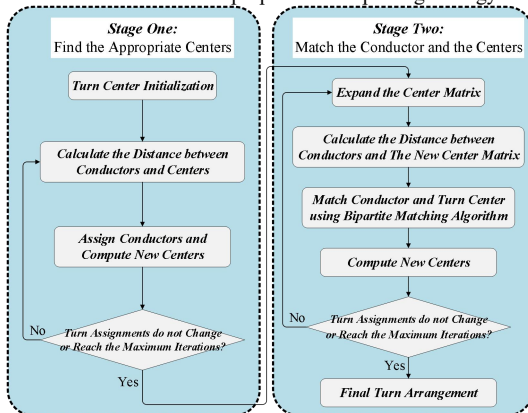


Fig. 6. The flowchart of the proposed turn splitting strategy.

The overall process is to find the appropriate center of each turn in the first stage (1-5), and match the conductor and the centers in the second stage (6-10) to make the conductors in each turn relatively concentrated. After the above process, the conductors in the slot can be divided into  $k$  turns with relatively concentrated distribution and the same number. The numbering rule for each strand in each turn is: from left to

right, and from the slot bottom to the slot opening.

Apply the proposed strategy to the studied machine and compare with the tangential one, the two different arrangements are shown in Fig. 7. It can be seen that due to the relatively small slot width, **the bundle shape of each turn and its conductor have little change.**

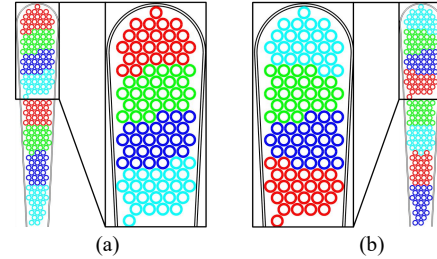


Fig. 7. Two different arrangements of the studied machine with 48-slot 4-pole. (a) Tangential arrangement. (b) Proposed arrangement.

To reflect the advantages of the proposed strategy, the number of slots of the studied machine is reduced from 48 to 24 to increase the slot width. On the premise that the conductor specification and slot filling factor remain unchanged, the number of conductors in the slot is increased. The voltage is kept constant by adjusting the number of turns. Finally, the number of parallel strands and turns of the machine with 24-slot is 29 and 8, respectively.

The conductor model and the two different arrangements are shown in Fig. 8. Due to the arrangement of the conductors in the same turn is the easiest, Fig. 8(a) is commonly used. However, **it is evident that** it does not closely represent the actual situation when the slot width is relatively large. The proposed arrangement which is shown in Fig. 8(b) gathers the conductors of the same turn together, making it more consistent with the actual distribution of conductors in the slot. However, it is more complicated, which makes it almost impossible to model in commercial FEM. **In contrast, the proposed method not only efficiently achieves the proposed arrangement, but also can greatly reduce modeling time and has better flexibility.**

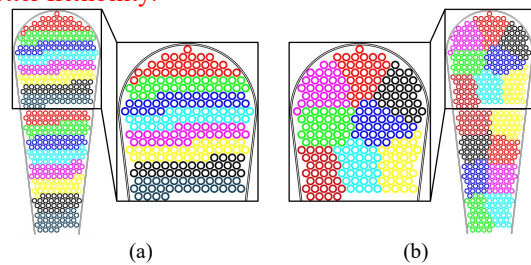


Fig. 8. Two different arrangements of the machine with 24-slot 4-pole. (a) Tangential arrangement. (b) Proposed arrangement.

### B. Slot Leakage Calculation by Time-Space Transformation Based FEM

**Once the conductor position information is obtained, the slot leakage of the conductors can be extracted using the CE FEM method, which can significantly reduce the computing time.**

The electric and magnetic circuit of an AC machine powered by sinusoidal current has time and space symmetry [24] [25]. According to this property, the full-period magnetic field waveform at a certain point can be reconstructed from a

shorter period waveform. The temporal and spatial distribution of the magnetic field in the machine stator slot can be expressed as:

$$A(t, \theta) = \sum_{v=1}^{\infty} A_v \sin(v\omega t - vp\theta + \gamma) \quad (1)$$

where  $t$  is the time,  $\theta$  is the position angle of the rotor,  $v$  is the order of the harmonics,  $\omega$  is the electrical radians per second,  $p$  is the pole pairs and  $\gamma$  is the phase angle. If the position angle changes, the following expression can be obtained:

$$\begin{aligned} A(t, \theta) &= \sum_{v=1}^{\infty} A_v \sin(v\omega t - vp(\theta + k\theta_s - k\theta_s) + \gamma) \\ &= \sum_{v=1}^{\infty} A_v \sin(v\omega t - vpk\theta_s - vp(\theta - k\theta_s) + \gamma) \\ &= \sum_{v=1}^{\infty} A_v \sin\left(v\omega\left(t - \frac{pk\theta_s}{\omega}\right) - vp(\theta - k\theta_s) + \gamma\right) \\ &= A\left(t - \frac{pk\theta_s}{\omega}, \theta - k\theta_s\right) \end{aligned} \quad (2)$$

Finally, we can get:

$$A\left(t + \frac{kp\theta_s}{\omega}, \theta\right) = A(t, \theta - k\theta_s) \quad (3)$$

Considering  $\omega = 2\pi/T$ , where  $T$  is the time of a period, the expression can be written as:

$$A\left(t + \frac{kp\theta_s T}{2\pi}, \theta\right) = A(t, \theta - k\theta_s) \quad (4)$$

where  $\theta_s$  is the slot pitch angle in mechanical measure, and  $k$  is an integer depends on the slots and poles of the machine. The value of  $k$  satisfies the following equation:

$$kp\theta_s = k_1\theta_{winding} \quad (5)$$

where  $\theta_{winding}$  is the angle between any two vectors in winding sequence diagram,  $k_1$  is a nonzero integer that make the above equation holds. Therefore, the minimum value of  $k$  is:

$$k_{min} = \frac{\theta_{winding}}{GCD(p\theta_s, \theta_{winding})} \quad (6)$$

Finally,  $k = n \times k_{min}$  ( $n = 0, 1, 2, \dots$ ).

Using the property, we only need to reconstruct the magnetic field of the first half of the period and the second half of the period is the opposite. From expression (4) and (5), it can be seen that the simulation time is related to  $\theta_{winding}$ . For example, for three-phase machines,  $\theta_{winding} = \pi/3$ , it is necessary to simulate only one sixth of the period, and  $n$  is from 0 to 2 which means that the magnetic fields at the same position in the three slots should be extracted at the same time to reconstruct the magnetic field we need.

For the investigated machine in this paper, the power supply mode is dual three-phase and the two sets of windings differ by  $\pi/6$  electrical angle which is shown in Fig. 1. Therefore,  $\theta_{winding} = \pi/6$ , and the simulation time can be one twelfth of the period,  $n$  is from 0 to 5 which means six slots are needed to reconstruct the magnetic field. If we want to reconstruct the vector potential of a conductor in phase A, according to expression (4), the following expressions can be obtained:

$$\begin{aligned} A_{a+}(t, \theta) &= A_{a+}(t, \theta), 0 \leq t < \frac{T}{12} \\ A_{a+}\left(t + \frac{T}{12}, \theta\right) &= A\left(t, \theta - \frac{\pi}{6 \times p}\right) = A_{x+}(t, \theta), 0 \leq t < \frac{T}{12} \\ A_{a+}\left(t + \frac{2T}{12}, \theta\right) &= A\left(t, \theta - \frac{\pi}{6 \times p} \times 2\right) = A_{b-}(t, \theta), 0 \leq t < \frac{T}{12} \\ A_{a+}\left(t + \frac{3T}{12}, \theta\right) &= A\left(t, \theta - \frac{\pi}{6 \times p} \times 3\right) = A_{y-}(t, \theta), 0 \leq t < \frac{T}{12} \\ A_{a+}\left(t + \frac{4T}{12}, \theta\right) &= A\left(t, \theta - \frac{\pi}{6 \times p} \times 4\right) = A_{c+}(t, \theta), 0 \leq t < \frac{T}{12} \\ A_{a+}\left(t + \frac{5T}{12}, \theta\right) &= A\left(t, \theta - \frac{\pi}{6 \times p} \times 5\right) = A_{z+}(t, \theta), 0 \leq t < \frac{T}{12} \end{aligned} \quad (7)$$

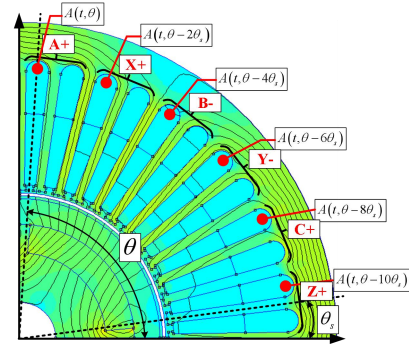


Fig. 9. The topology and slot location of the studied machine.

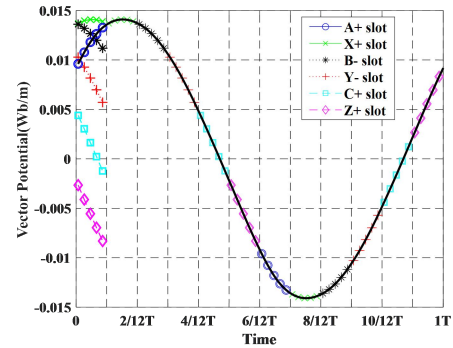


Fig. 10. Reconstruction of the vector potential in the A+ slot.

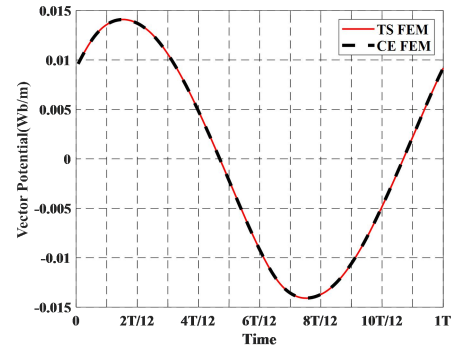


Fig. 11. Comparison between CE FEM and TS FEM.

It means we can use the magnetic field of A+, X+, B-, Y-, C+ and Z+ slots, respectively, in one twelfth of the period to reconstruct the magnetic field of a complete period. The machine topology and slot location are shown in Fig. 9. The extracted magnetic field in the center of the first conductor in

one twelfth period and the reconstructed waveform in the full period are shown in Fig. 10. The comparison between reconstructed waveforms and the real waveforms in the full period is shown in Fig. 11. They are in good agreement, and it verifies the accuracy of CE FEM.

### C. Circuit Model and Circulating Current Loss Evaluation

For the parallel strands, the voltage equation is the following:

$$\begin{cases} U = I_1 R_1 + j\omega(L_1 I_1 + \dots + M_{1n} I_n + M_{1A} I_A + M_{1B} I_B + M_{1C} I_C) + j\omega\varphi_m = I_1 R_1 + j\omega\varphi_1 \\ U = I_2 R_2 + j\omega(M_{21} I_1 + \dots + M_{2n} I_n + M_{2A} I_A + M_{2B} I_B + M_{2C} I_C) + j\omega\varphi_m = I_2 R_2 + j\omega\varphi_2 \\ \vdots \\ U = I_n R_n + j\omega(M_{n1} I_1 + \dots + M_{nn} I_n + M_{nA} I_A + M_{nB} I_B + M_{nC} I_C) + j\omega\varphi_m = I_n R_n + j\omega\varphi_n \end{cases} \quad (8)$$

where  $U$  is the terminal voltage,  $I_1 \dots I_n$  are the currents in the parallel strands,  $L$  is the self-induction,  $M$  is the mutual-inductance,  $I_A$ ,  $I_B$  and  $I_C$  is the current in the phase,  $R$  is the DC resistance in each strand,  $\varphi_m$  is the flux linkage of the permanent magnet and  $\varphi_1 \dots \varphi_n$  represents the whole flux linkage of each strand.

Drawing on the idea of decomposition, the current of each strand is divided into the average current and the induced current which is shown in Fig. 12. The average current assumes that there is no circulating current between the parallel strands, and the total current in one turn is evenly distributed in each parallel strand. The induced current is caused by the change of the external magnetic field. Obviously, the average current is easily obtained, however, the induced current needs to be considered carefully.

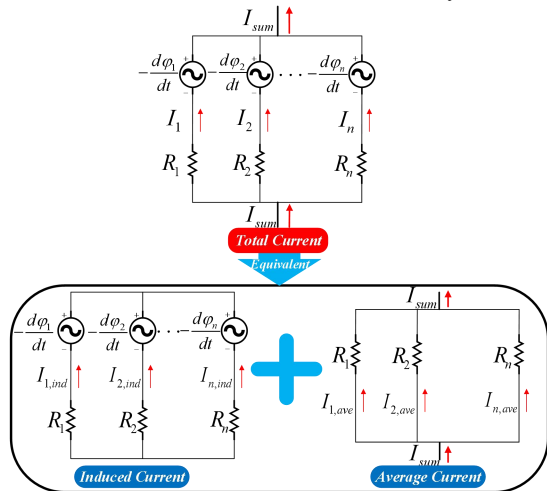


Fig. 12. The circuit model with  $n$  parallel strands.

In order to calculate the induced current, the winding circuit model is built as shown in Fig. 12 marked with induced current, there is no current input and the model contains one turn of winding with  $n$  parallel strands, each strand is modeled as a voltage source and a resistor in series. The voltage source of each strand is the induced electromotive force, which is caused by the change of flux linkage. By means of the voltage equation (8) in this section, the overall flux leakage in each strand results from the slot leakage and the conductors in the same slot. Based on the third assumption, the whole flux linkage can be obtained by the product of the vector potential at the center of the strand cross-section and the strand length, and it can be quickly obtained through CE FEM.

The induced current in each strand can be calculated separately. For example, in order to calculate the induced current in the  $k$ th strand, the other strands are equivalent to a model with a voltage source and a resistor in series which is shown in Fig. 13.

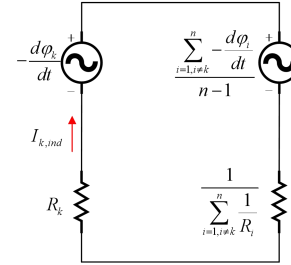


Fig. 13. Equivalent circuit model.

Then, the circuit equation can be obtained as shown in equation (9). In this equation, the DC resistance on the left side and the flux linkage on the right side are all known, therefore, the induced current in each strand can be solved.

$$I_{k,ind} \times \left( R_k + 1 / \left( \sum_{i=1, i \neq k}^n \frac{1}{R_i} \right) \right) = - \frac{d\varphi_k}{dt} + \sum_{i=1, i \neq k}^n \frac{d\varphi_i}{dt} / (n-1) \quad (9)$$

Finally, the total current in the  $k$ th strand is:

$$I_k = I_{k,ind} + I_{k,ave} \quad (10)$$

After getting the current of each strand, the circulating current loss can be calculated:

$$P_{closs} = \sum_{i=1}^n (I_i^2 - I_{i,ave}^2) R_i \quad (11)$$

### D. Comparison between Commercial FEM and Proposed Method.

In order to verify the accuracy of the proposed method, the results are compared with the commercial finite element software ANSYS Maxwell 2015. It is worth noting that the power loss of the results in this section and next section (section IV) is defined by equation (12), which includes DC copper loss  $P_{DCcopperloss}$  and circulating current loss, however, the definition in section V has slight differences and a detailed explanation will be provided in section V.

$$P_{loss} = P_{closs} + P_{DCcopperloss} \quad (12)$$

The results of the two arrangements for the studied machine with 48-slot calculated by the commercial FEM and the proposed method are shown in Fig. 14. On the one hand, the frequency is from 200Hz to 1800Hz, and the loss of the two arrangements increases sharply, however, the error between two methods still very small. When the frequency reaches 1800Hz, the error of the two arrangements calculated by the two methods is less than 2%, and the proposed method is bigger than the commercial FEM. That is because the proposed method neglects the reaction of the circulating current and the influence of the unequal current distribution to the external magnetic field. On the other hand, for the studied machine with 48-slot, the slot width is relatively small, and the difference of circulating current loss between the two arrangements is very small, leading to similar power loss, which is also can be seen from Fig. 7.

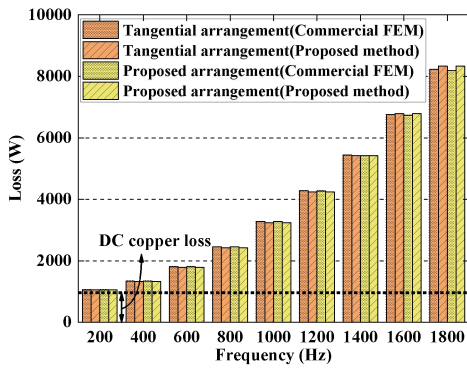


Fig. 14. Comparison of the power loss of the two arrangements between commercial FEM and proposed method for the machine with 48-slot.

When the frequency reaches 1800Hz, the currents of the tangential arrangement in some strands calculated by two methods are shown in Fig. 15, although the frequency is extremely high, the currents still show little difference, that is why the losses show good agreement. As the frequency continues to increase, it is expected that the error between the two methods will also increase. This is mainly because the increase in frequency causes an increase in circulating current loss, and the unbalanced current in the parallel strands will change the slot leakage, which makes a huge difference between the magnetic field extracted from the simple model and the actual magnetic field.

In addition, the proposed method has great advantages in computing time which is shown in Table II. Compared with 9000 seconds of commercial FEM, the proposed method only takes 22 seconds, which makes the computing efficiency 400 times higher. This means that the proposed method can be used to rapidly optimize the machine by considering AC copper loss at the initial stage of machine design.

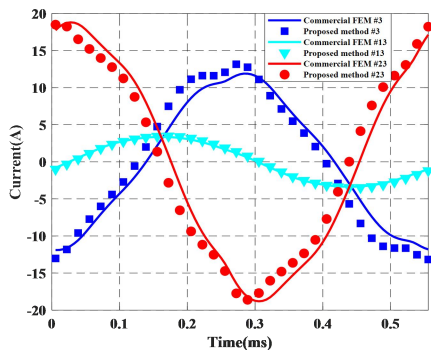


Fig. 15. Comparison of the currents for the machine with 48-slot between commercial FEM and proposed method (tangential arrangement, 1800Hz).

TABLE II  
COMPARISON OF TWO METHODS (Tangential, 1800Hz)

Method	Power loss	Error	Computation time
Commercial FEM	8232W	--	9000s
Proposed method	8340W	<2%	22s

For the machine with small slot width, the turn distribution of the proposed arrangement and the tangential arrangement shows little difference as shown in Fig. 7, resulting in a negligible difference in circulating current loss, as shown in Fig. 14. However, for the machine with large slot width, the turn distribution of the two arrangements has big difference as

shown in Fig. 8, which may lead to great difference in circulating current loss.

The proposed method and the commercial FEM are used to calculate the circulating current loss of the machine with 24-slot as shown in Fig. 8. The results for the two arrangements are shown in Fig. 16, it is evident that the bundle shape significantly impacts the circulating current loss. When the frequency reaches 1800Hz, based on the results calculated by the commercial FEM, the power loss of the tangential arrangement is 2950W, however, the proposed arrangement reaches 8530W, three times the difference between the two arrangements. The circulating current loss will be seriously underestimated when the conductors are arranged in tangential. This suggests that we should carefully select the split turn model when evaluating the circulating current loss, which has a huge impact on the circulating current loss. Meanwhile, in the case of the tangential arrangement, the maximum error between the two methods is 2%, and for the proposed arrangement, the maximum error is 7.58%. The reason is that the unbalanced current in the parallel strands has an influence on the slot leakage, resulting in an increased error in the extracted slot leakage, which the simple model fails to account for. Nevertheless, the proposed method maintains a high level of accuracy.

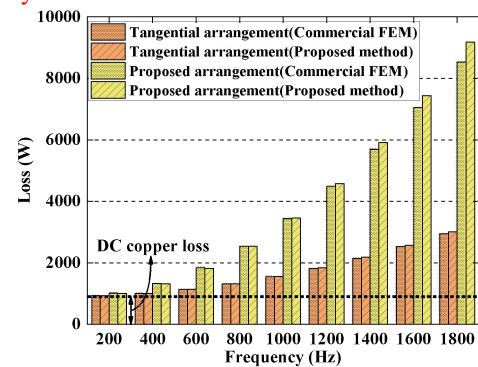


Fig. 16. Comparison of the power loss of the two arrangements between commercial FEM and proposed method for the machine with 24-slot.

#### IV. INFLUENCE FACTOR INVESTIGATION BY THE PROPOSED METHOD

##### A. The Influence of Different Bundle/Turn Combination on the Circulating Current Loss

The influence of different bundle/turn combination will be investigated in this section using three machines. The geometry, the number of slots and poles of the three machines are the same as the studied machine, only the winding parameters are adjusted. The number of conductors per slot of the three machines is 96, due to the number of parallel strands is 16, 24 and 32, the number of turns per coil is 6, 4 and 3, respectively. The strands in the same turn are numbered from left to right, from slot bottom to slot opening. In order to keep the electromagnetic environment of the machine consistent, the phase current needs to be changed according to the number of turns, hence, the rated current per phase is 150Arms, 225Arms and 300Arms, respectively. The winding parameters of the three machines are shown in Fig. 17 and Table III.

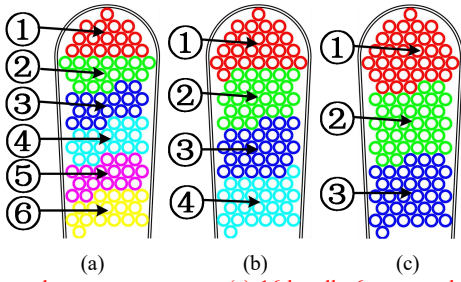


Fig. 17. The conductor arrangements. (a) 16-bundle 6-turn machine. (b) 24-bundle 4-turn machine. (c) 32-bundle 3-turn machine.

TABLE III  
WINDING PARAMETERS OF THE THREE MACHINES

Parameters	A	B	C
Number of turns per coil	6	4	3
Strands-in-hand	16	24	32
Rated current per phase (A. rms)	150	225	300
Line to line voltage (V)	460	310	230

The power loss including circulating current loss and the DC copper loss is shown in Fig. 18. It can be seen that the power loss increases rapidly as the number of parallel strands increases. When the frequency reaches 1800Hz, the power loss of the machine with 16 parallel strands is only 4417W, the machine with 24 parallel strands is 8483W, however, the machine with 32 parallel strands reaches 13365W, the reason is that the magnetic line is parallel to the bottom of the slot, the more parallel strands, the longer the distance of the same turn, which leads to a larger gap in the slot leakage between parallel strands and the bigger circulating current loss. Meanwhile, it can be seen that for the machines with the same ampere-turns, the greater the current, the greater the circulating current loss. Therefore, we should pay special attention when designing winding parameters. On the other hand, the maximum error of the three combinations between the two methods are 1%, 3% and 11%, respectively. That's also because with the increase of the circulating current loss, the influence of the unbalanced current in the strands on the slot leakage becomes more and more significant, however, the simple model can't reflect the influence. Nevertheless, the error of 11% at the frequency of 1800Hz is also very considerable.

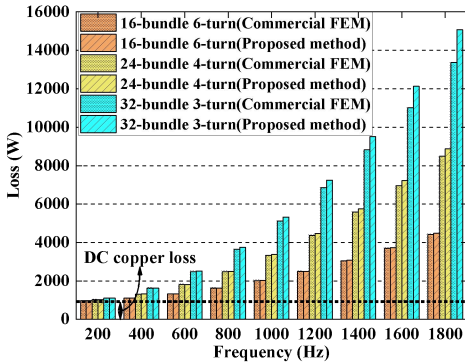


Fig. 18. Comparison of the power loss of the three machines between the commercial FEM and the proposed method.

### B. The Influence of Transposition on the Circulating Current Loss

Coil transposition has great influence on circulating current loss, and a transposition technique is studied using the proposed

method. As mentioned earlier, the studied machine has two coils in a parallel branch. When transposition is not used, the conductor indexes in the same turn of the two coils are the same as shown in the Fig. 19(a). After using the transposition technology, the conductor indexes are shown in the Fig. 19(b), which means there is 180° transposition between the two coils.

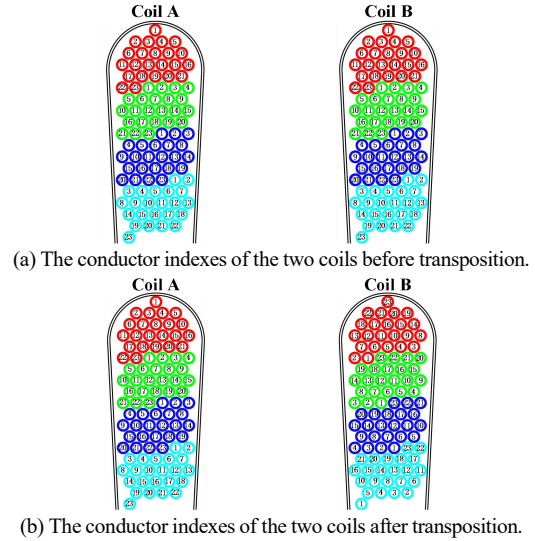


Fig. 19. The conductor indexes (a) before transposition and (b) after transposition.

The results including circulating current loss and the DC copper loss calculated by the two methods before and after transposition are shown in Fig. 20. It can be seen that the transposition greatly reduced the circulating current loss, which makes the power loss decreases from 8232W to 1047W, almost 87% when the frequency reaches 1800Hz. The transposition technique can effectively reduce circulating current loss. Meanwhile, the maximum error between the two methods is both less than 2%, which verifies the effectiveness of the proposed method.

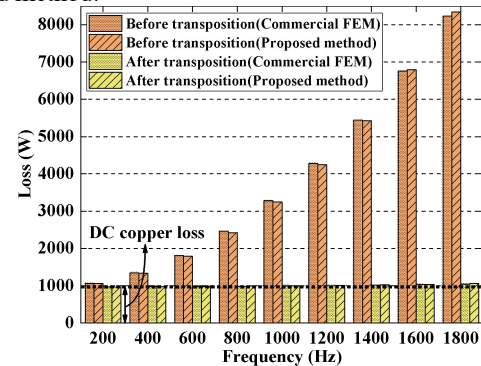


Fig. 20. Comparison of the power loss before and after transposition between the commercial FEM and the proposed method.

### C. The Influence of the Bundle Shape on the Circulating Current Loss

The bundle shape inside the slot is usually uncertain. In order to generate more bundle shapes, assuming that the y-axis is at the centerline of the slot, and a weighted parameter  $w$  is added to the distance calculation in the turn splitting strategy in section III. A. Therefore, the weighted distance can be calculated as shown in equation (13):

$$d_{ij} = \sqrt{(x_i - x_j)^2 + w^2(y_i - y_j)^2} \quad (13)$$

where  $d_{ij}$  is the weighted distance between two conductors,  $x, y$  is the coordinates of the conductors. Using this weighted distance, more elliptical-like bundle shapes can be generated, and the bundle shapes for the machine with 48-slot are shown in Fig. 21. The parameter changes from 0 to 10, and the bundle shapes can change from radial (worst) to tangential (best). The strands in the same turn are numbered from top to bottom, from left to right.

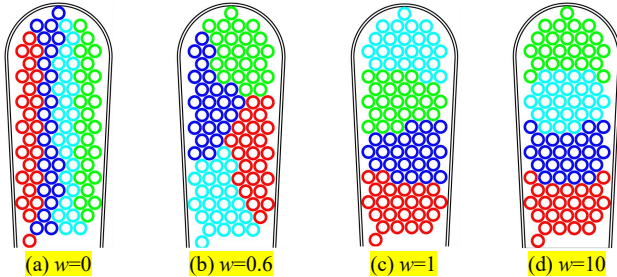


Fig. 21. Elliptical-like bundle shapes for the studied machine with 48-slot.

The results including circulating current loss and the DC copper loss calculated by the two methods are shown in Fig. 22. It can be seen that as  $w$  decreases, the bundle shape tends to be more radial, resulting in a significant increase in circulating current loss. When the frequency is 1800Hz, based on the results calculated by the commercial FEM, the power loss at  $w=0$  is more than twice as much as  $w=1$ , and the power loss at  $w=0.6$  is approximately 1.4 times that of  $w=1$ . In addition, the error between the commercial FEM and the proposed method increases as  $w$  decreases. When the frequency is 1800Hz, the error is about 15% at  $w=0.6$ , however, the error reaches 437% at  $w=0$ , which is unacceptable. The reason for this is that as  $w$  decreases, the bundle shape tends to be more radial, resulting in a larger difference in the flux linkage of the strands in the same turn, thereby significantly increasing the circulating current. The largely increased circulating current will non-negligibly affect the slot leakage in turn, which is inconsistent with the second assumption of the proposed method. Therefore, the proposed method is not suitable for the extreme situations, where the turn is radially arranged or occupies a large area. Even though, it can serve as a useful tool to estimate the circulating loss quickly in large-scale optimization process for most machine designs.

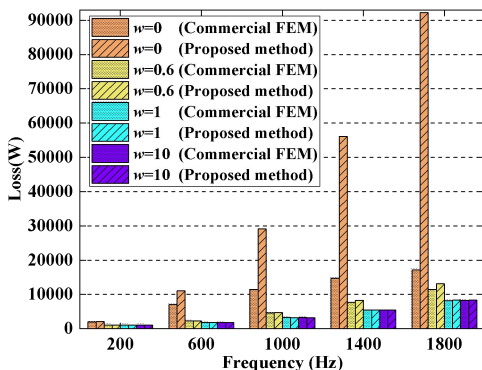


Fig. 22. Comparison of the power loss of different bundle shapes between the commercial FEM and the proposed method for the studied machine with 48-slot.

## V. EXPERIMENTAL VALIDATION

The rotor induced AC copper loss for the machine with half-closed slots is usually not significant [14]. To get rid of the hardly determined rotor PM loss and bearing loss, thus reducing the validation difficulty, the validation of the proposed method was conducted on two stator specimens. Since the circulating current in the parallel strands is greatly affected by the conductor position, the first stator specimen adopts the molds made of FR-4 epoxy glass cloth to fix the conductor position in the slot. In this case, the influence of conductor position can be ruled out, and the measured currents can be well used to validate the CE FEM based circulating current calculation method. Furthermore, a second stator specimen with the randomly wound windings is used to validate the proposed turn splitting strategy, aiming at illustrating the practicability of the proposed method.

### A. Verification of Circulating Current Loss with Fixed Conductor Position

The first stator specimen and the component of the experiment platform are shown in Fig. 23. The molds and the indexes of the conductors in the slot are shown in Fig. 23(b), Fig. 23(d), respectively. The number 1-4 represent the four parallel strands, and the parallel strands in the same turn has the same color. The power source uses the AC power supply (ITECH 7625), and it supplies 10Arms sinusoidal current to the coil. The resistance of each parallel strand is measured by the precise digital micro ohmmeter (SEAWARD DO7). The measuring instrument uses an oscilloscope with the current probe (RS&RTZC 20) to measure the current in the parallel strands.

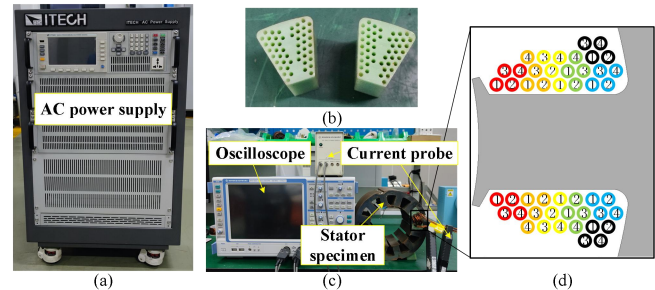


Fig. 23. The component of the experiment platform. (a) The AC power supply. (b) The molds made of FR-4 epoxy glass cloth. (c) The measuring instruments. (d) The indexes of the conductors.

Fig. 24 shows the comparison of the current between the proposed method and the experiment, the magnitude and angle of the arrow are used to represent the amplitude and phase of the current. It can be seen that the error of the currents in the parallel strands between the proposed method and the experiment are very small. The error between them increases as the frequency increases, when the frequency reaches 1600Hz, the maximum error of the amplitude between them reaches 16%, the error of the phase is  $\pi/20$ .

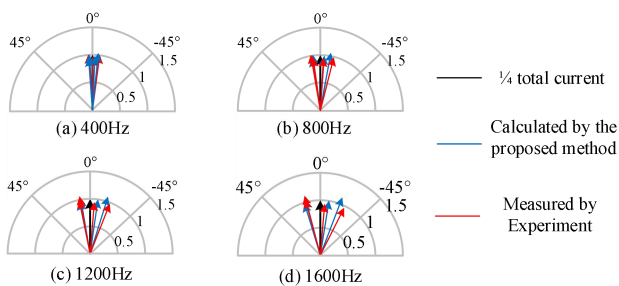


Fig. 24. Comparison of the currents between the proposed method and the experiment.

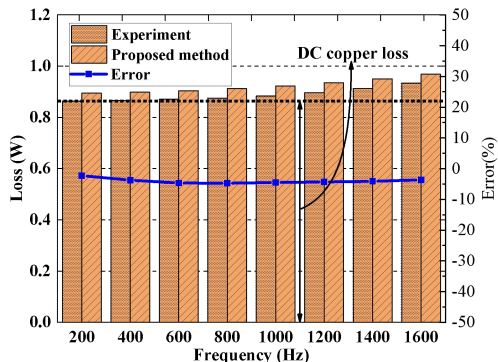


Fig. 25. Comparison of the power loss between the proposed method and the experiment.

The comparison of the power loss between the proposed method and the experiment is shown in Fig. 25. The currents and the circulating current loss in the parallel strands can be directly obtained, therefore, the power loss is also defined by Equation (12). The maximum error between the experiment and the proposed method is 4.74% at 800Hz. This experiment avoids the influence of conductor position on circulating current loss, verifying the accuracy of the proposed CE FEM.

### B. Verification of Circulating Current Loss with Randomly Wound Windings

To verify the effectiveness of the proposed method for calculating the circulating current loss of the mass-produced machine, a stator specimen with two randomly wound coil groups of the studied machine is manufactured which is shown in Fig. 26(a). Each coil group includes two coils. Different from the above experiment, each coil group of the stator specimen is manually wound in a practical manner which leads to randomness of conductor position.

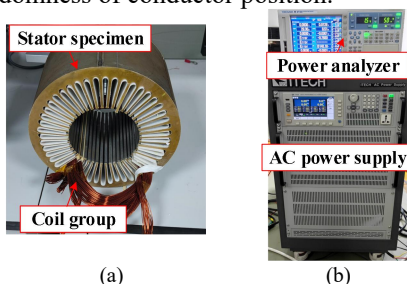


Fig. 26. The component of the experiment platform. (a) The stator specimen with randomly wound coil groups. (b) The instruments.

Fig. 26(b) shows the instruments of the experiment platform. The AC power supply (ITECH 7625) is also used to supply 10Arms sinusoidal current to the windings. A power analyzer (WT1800) is used to measure the total loss in the stator specimen, which includes the core losses, the eddy

current loss within the strands and the circulating current loss between the parallel strands. Due to the large number of randomly located strands, it is difficult to directly obtain the circulating current loss based on the measured strand currents. To validate the proposed method, the different loss components have to be separated.

The core losses are calculated by the commercial FEM using the measured magnetic characteristics ( $B$ - $H$  curves) and the specific core loss data ( $B$ - $P$  curves). The strand eddy current loss is calculated using the method proposed in [3]. Based on the above calculations, the experimental and calculated total copper loss can be obtained as following equation:

$$P_{loss\_exp} = P_{totalloss} - P_{corelosses} \quad (14)$$

$$P_{loss\_prop} = P_{ccloss} + P_{DCcopperloss} + P_{eddyloss}$$

where  $P_{totalloss}$  is the total loss measured in the experiment,  $P_{corelosses}$  is the core losses simulated by the commercial FEM,  $P_{eddyloss}$  is the eddy current loss of the conductors in the slot.

The total copper losses calculated by the proposed method and measured by the experiment are shown in Fig. 27. It can be seen that the results of the proposed method are very close to the experimental results. The maximum error between the proposed method and the experiment is 21% at 200Hz, 16% at 1800Hz in coil group 1 and 21% at 200Hz, 14% at 1200Hz in coil group 2. Anyway, the proposed method still leads a satisfactory result for the circulating current loss of randomly wound windings, and verifies that it can be used for rapid assessment of circulating current loss.

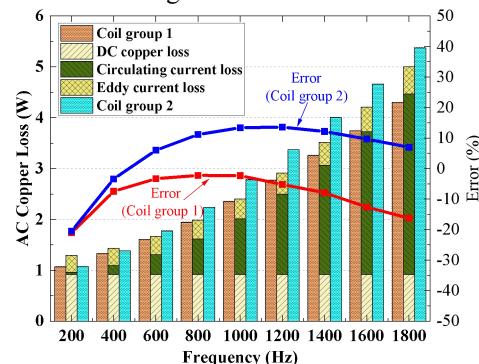


Fig. 27. Comparison of the AC copper loss between the proposed method and the experiment.

## VI. CONCLUSION

A CE semi-analytical method which combines the CE static FEM and an analytical circuit model is proposed for circulating current loss calculation in this paper. Time-space transformation based CE FEM is first applied for slot leakage field calculation to reduce the computation cost. It shows that the saving time depends on the winding patterns and the simulation time can be further reduced to 1/12 compared to the conventional FEM for the investigated dual three-phase winding with phasor difference angle of  $\pi/6$ . Besides, a conductor model with an automatic and practical turn splitting strategy is proposed to establish a circuit model considering the actual coil structure, in which the conductors belonging to the same turn tend to be concentrated. Therefore, the proposed

turn splitting strategy has good applicability to machines with either narrow or wide slots.

The calculated loss results match well with the FEM results with errors less than 2% over a wide frequency range while the simulation time is only 1/400 for the studied machine. The proposed method is applied to investigate the effects of turn number, transposition and the bundle shape on the circulating current loss, which further validates its accuracy and applicability. Finally, the proposed method was validated by experiments implemented on two stator specimens.

The proposed method provides a useful tool featuring both accuracy and efficiency for circulating current loss calculation. Even though it has limitations in calculating the circulating loss for some rarely emerged extreme situations where the turn is radially arranged or occupies a large area, it can serve as a useful tool to estimate the circulating loss quickly in large-scale optimization process for most machine designs. In future work, the impact of the randomness of conductor position on the circulating current loss will be explored and the machine will also be optimized considering the AC copper loss based on the proposed method. The overall objective is to achieve the balance between power density and efficiency considering the AC copper loss and thermal aspect.

#### REFERENCES

- [1] D. Golovanov, L. Papini, D. Gerada, Z. Xu, and C. Gerada, "Multidomain optimization of high-power-density PM electrical machines for system architecture selection," *IEEE Trans. Ind. Electron.*, vol. 65, no. 7, pp. 5302-5312, Jul. 2018.
- [2] T. Iida, M. Takemoto, S. Ogasawara, K. Orikawa, I. Sato, H. Kokubun, A. Toba, and M. Syuto, "Investigation of enhancing output power density in ultra-high-speed motors with concentrated winding structure," in *Proc. IEEE Energy Convers. Congr. Expo.*, 2020, pp. 1-8.
- [3] X. Fan, D. Li, W. Kong, L. Cao, R. Qu, and Z. Yin, "Fast calculation of strand eddy current loss in inverter-fed electrical machines," *IEEE Trans. Ind. Electron.*, vol. 65, no. 7, pp. 4640-4650, May/2023.
- [4] X. Fan, D. Li, R. Qu, C. Wang, and C. Chen, "Effect of AC losses on temperature rise distribution in concentrated windings of permanent magnet synchronous machines with parallel strands," in *Proc. IEEE Int. Conf. on Elect. Mach. and Syst. (ICEMS)*, Sydney, NSW, 2017, pp. 1-6.
- [5] R. Wrobel, A. Mlot, and P. H. Mellor, "Contribution of end-winding proximity losses to temperature variation in electromagnetic devices," *IEEE Trans. Ind. Electron.*, vol. 58, no. 2, pp. 848-857, 2011.
- [6] A. Lehtikoinen, N. Chioldetto, E. Lantto, A. Arkkio and A. Belahcen, "Monte Carlo analysis of circulating currents in random-wound electrical machines," *IEEE Trans. Magn.*, vol. 52, no. 8, pp. 1-12, Aug. 2016.
- [7] M. Popescu and D. G. Dorrell, "Proximity losses in the windings of high speed brushless permanent magnet ac motors with single tooth windings and parallel paths," *IEEE Trans. Magn.*, vol. 49, no. 7, pp. 3913-3916, Jul. 2013.
- [8] F. Birkammer, J. Chen, D. Bachinski Pinhal and D. Gerling, "Influence of the modeling depth and voltage level on the AC losses in parallel conductors of a permanent magnet synchronous machine," in *IEEE Trans. on Appl. Super.*, vol. 28, no. 3, pp. 1-5, April 2018.
- [9] A. Bardalai et al., "Reduction of winding AC losses by accurate conductor placement in high frequency electrical machines," *IEEE Trans. Ind. Appl.*, vol. 56, no. 1, pp. 183-193, Jan./Feb. 2020.
- [10] J. Liu, X. Fan, D. Li, R. Qu and H. Fang, "Minimization of AC copper loss in permanent magnet machines by transposed coil connection," *IEEE Trans. Ind. Appl.*, vol. 57, no. 3, pp. 2460-2470, May/June. 2021.
- [11] X. Chen, H. Fang, X. Fan, H. Hu, D. Li and R. Qu, "Suppression of winding AC copper loss in high-speed electrical machines by a practical transposition technique," *IEEE Trans. Ind. Appl.*, vol. 58, no. 6, pp. 7121-7130, Nov/Dec. 2022.
- [12] P. B. Reddy, T. M. Jahns, and T. P. Bohn, "Modeling and analysis of proximity losses in high-speed surface permanent magnet machines with concentrated windings," in *Proc. IEEE Energy Convers. Congr. Expo.*, 2010, pp. 996-1003.
- [13] Y. Jiang, J. Chen, H. Wang and D. Wang, "Semi-analytical method of form-wound winding loss considering circulating current effect," *IEEE Trans. Magn.*, vol. 58, no. 2, pp. 1-6, Feb. 2022.
- [14] D. Golovanov and C. Gerada, "Analytical methodology for modelling of circulating current loss in synchronous electrical machines with permanent magnets," *IEEE Trans. Energy Convers.*, vol. 37, no. 1, pp. 220-231, Mar. 2022.
- [15] S. Xu and H. Ren, "Analytical computation for AC resistance and reactance of electric machine windings in ferromagnetic slots," *IEEE Trans. Energy Convers.*, vol. 33, no. 4, pp. 1855-1864, Dec. 2018.
- [16] G. Artetxe, B. Prieto, D. Caballero, I. Elosegui and G. M. Maza, "A practical approach for estimating bundle-level proximity losses in AC machines," *IEEE Trans. Ind. Electron.*, vol. 69, no. 12, pp. 12173-12181, Dec. 2022.
- [17] M. van der Geest, H. Polinder, J. A. Ferreira, and D. Zeilstra, "Current sharing analysis of parallel strands in low-voltage high-speed machines," *IEEE Trans. Ind. Electron.*, vol. 61, no. 6, pp. 3064-3070, Jun. 2014.
- [18] Y. Jiang, J. Chen, X. Teng, and D. Wang, "Circulating current analysis for high-speed motors with stranded windings by considering end and temperature effect," *J. Magn. Magn. Mater.*, vol. 23, no. 4, pp. 659-664, 2018.
- [19] G. Volpe, M. Popescu, F. Marignetti, and J. Goss, "AC winding losses in automotive traction e-Machines: a new hybrid calculation method," *2019 IEEE International Electric Machines & Drives Conference (IEMDC)*, pp. 1-5.
- [20] C. Roth, F. Birkammer and D. Gerling, "Analytical model for ac loss calculation applied to parallel conductors in electrical machines," *2018 XIII International Conference on Electrical Machines (ICEM)*, pp. 1088-1094, 2018.
- [21] D. Meeker, Finite Element Method Magnetics (FEMM), Version 4.2.
- [22] ZhiYong Zhang. MATLAB TUTORIAL. BEIHANG University Publishing Company. 2006.8.
- [23] Duff, Iain S., and Jacko Koster, "On algorithms for permuting large entries to the diagonal of a sparse matrix," *SIAM J MATRIX ANAL A*, vol 22, no. 4, pp. 973-996, 2001.
- [24] G. Y. Sizov, "Design synthesis and optimization of permanent magnet synchronous machines based on computationally-efficient finite element analysis," 2013.
- [25] D. M. Ionel and M. Popescu, "Ultrafast finite-element analysis of brushless PM machines based on space-time transformations," *IEEE Trans. Ind. Appl.*, vol. 47, no. 2, pp. 744-753, Mar. 2011.